

35. MEASUREMENT OF HEAT FLOW ON LEG 86 OF THE DEEP SEA DRILLING PROJECT¹

Ki-iti Horai, Lamont-Doherty Geological Observatory of Columbia University
and

R. P. Von Herzen, Woods Hole Oceanographic Institution²

ABSTRACT

Using a new temperature recording instrument recently developed at the Woods Hole Oceanographic Institution, downhole temperature measurements were made at five sites during Deep Sea Drilling Project Leg 86. The instrument, which can be installed in the shoe of the hydraulic piston corer, allows measurements of sediment temperature to be made simultaneously with the collection of sediment cores. A numerical procedure was applied to correct the temperature disturbance caused by the corer's friction with the sediment. Detailed temperature profiles constructed from the data were combined with the measurement of thermal conductivity to calculate heat flow. Heat flow values were generally low at all sites of Leg 86, consistent with the age of the lithosphere (≥ 100 m.y.) in the Northwestern Pacific Basin.

INTRODUCTION

Since the earliest phase of the Deep Sea Drilling Project (DSDP), measurement of heat flow has been one of the major objectives of the project. The DSDP heat flow program was initiated by Burns (1970) on Leg 5 and was continued by Von Herzen et al. (1971) on Leg 8. Following these preliminary experiments, a self-contained heat flow instrument was developed at the Woods Hole Oceanographic Institution (WHOI). A series of successful measurements were obtained on Leg 19 (Erickson, 1973) and subsequent legs until Leg 46 (Von Herzen, 1973; Sclater and Erickson, 1974; Girdler et al., 1974; Marshall and Erickson, 1974; Hyndman et al., 1974; Watanabe et al., 1975; Hyndman et al., 1977; Erickson and Hyndman, 1979), except for occasional renovations to the instrumentation.

The program was revitalized by Uyeda and Horai (1982) on Leg 60 using a new solid-state recording temperature probe developed by the Earthquake Research Institute of the University of Tokyo (Yokota et al., 1980), and several successful measurements ensued. Overall, however, the opportunity of fully utilizing a deep-drilled DSDP hole for the purpose of heat flow study has not been realized.

The primary obstacle that prevented extensive use of deep-sea drilling holes for heat flow studies lay in the method of using the heat flow instrumentation. Drilling and coring had to be halted for 1 to 2 hr. to lower the heat flow instrument into the drilled hole and take a temperature measurement. A hiatus in the core sampling program for sediment temperature measurements proved intolerable to many shipboard scientists eager to gather and analyze sediment samples.

A new temperature recording instrument developed at the Woods Hole Oceanographic Institution in 1982 is much improved in that respect. Its miniature size enabled it to be inserted into the cutting shoe of the hydraulic piston corer (HPC). This allowed sediment temperatures to be measured simultaneously with the core sampling procedure. The instrument was tested and used for the first time on Leg 86; this chapter summarizes the data and results from that leg.

TEMPERATURE MEASUREMENT METHOD

Figure 1 illustrates the shoe of the HPC that contains the temperature recording instrument. The instrument consists of a temperature sensor, a recorder, and a battery pack that are installed in the slots located in the wall of the shoe. The temperature sensor is a thermistor encased in a stainless steel tube of 3-mm diameter with a tip smeared with heat sink compound to ensure thermal contact with the wall. The recorder is a preprogrammable miniature computer (microprocessor), energized by the battery pack, with memory for storing the measured temperature data. Prior to the coring operation, the recorder is connected to a shipboard computer. Parameters such as the starting time of the recorder, the time interval between measurements, and the total number of measurements are loaded as a command. The computer is disconnected and the recorder then proceeds to execute the program as specified by the parameters. Upon completion of the coring operation, the recorder is recovered along with the HPC core, removed from the HPC shoe, and connected to the computer again to dump the data. The data are then ready for visual display and the numerical analysis required to obtain undisturbed *in situ* temperatures.

Temperature measurements were made at all sites except Site 581 during Leg 86. The HPC was equipped with the temperature recording instrument and lowered in the drill hole every few cores to obtain data at intervals appropriate for delineating a sediment temperature pro-

¹ Heath, G. R., Burckle, L. H., et al., *Init. Repts. DSDP*, 86: Washington (U.S. Govt. Printing Office).

² Addresses: (Horai, present address) Meteorological College, Asahicho, Kashiwa. Chiba 277, Japan; (Von Herzen) Woods Hole Oceanographic Institution, Woods Hole, MA 02543.

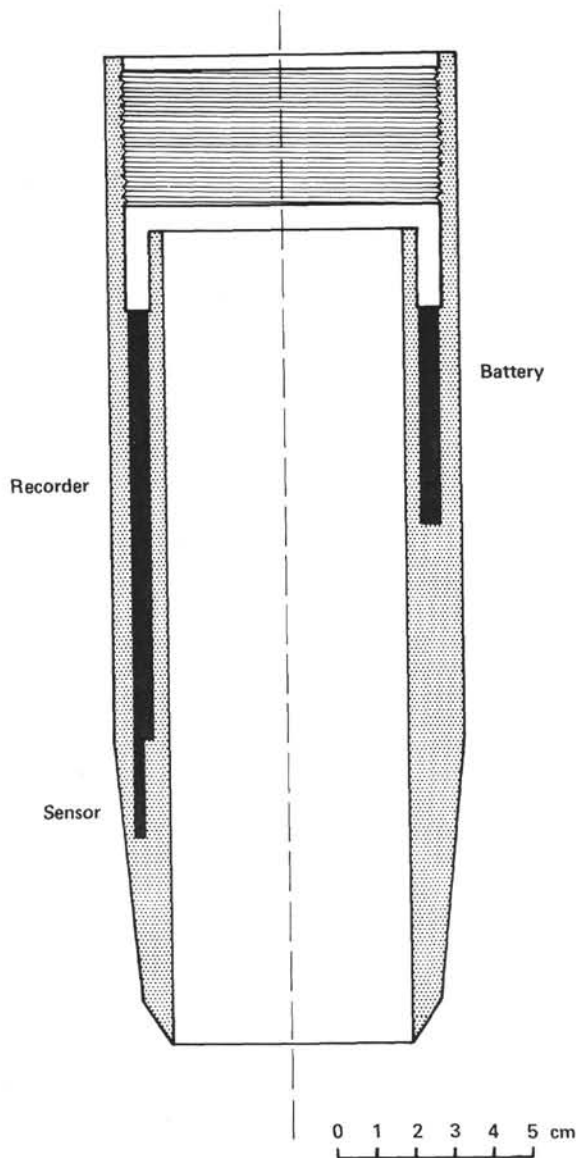


Figure 1. Shoe of the HPC equipped with temperature recorder, sensor, and battery pack.

file. For most instruments, the recorder was programmed so that sediment temperature values were recorded every 20 s while the instrument was in the sediment. The recorded sediment temperature data contain a disturbance that results from frictional heating to which the HPC is subjected as it is thrust into the sediment. This disturbance component in the data is removed numerically to obtain an estimate of undisturbed sediment temperature.

DATA ANALYSIS

Figure 2 shows the temperature data collected from Core 578-14, which was one of the best examples from Leg 86. As the temperature sensor of the recording device was placed within 5 mm of the outer surface of the metallic (thermal conductive) HPC, the measured temperature reflected the changing thermal environment

around the HPC due to the conduction of frictional heating.

From a temperature record such as that obtained in Figure 2, the undisturbed sediment temperature can be estimated by the least-square fitting of a theoretical cooling curve to the portion of the temperature data showing the HPC's cooling (c in Fig. 2).

The theoretical cooling curve was obtained by solving the thermal conduction equation for composite circular cylinders simulating the HPC in the sediment (Fig. 3). The HPC is subject to frictional heating as it thrusts into the sediment. The heat of friction between the HPC and the sediment is partly accumulated in the HPC and reaches a maximum when the penetration is completed and the HPC comes to a stop. The distribution of the frictional heat is not uniform in the HPC. Radially, the heating is restricted near the HPC's inner and outer boundaries where it contacts the sediment. Due to high thermal conductivity of the metal composing the HPC, it can be regarded radially isothermal after several tens of seconds of its penetration into the sediment. The thermal conduction equation was solved for the initial condition that, at time $t = 0$, temperature V is uniform in the HPC (middle cylinder) and is zero in the sediment (inner and outer cylinders). If the solution of this equation is obtained for $V = 1.0^\circ\text{C}$, its time dependence $V(t)$ evaluated at the outer boundary of the middle cylinder is the HPC's theoretical cooling temperature from an initial value of unity. The observed cooling curve is adequately described by a formula $\alpha V(t) + \beta$ with two adjustable constants α and β (Fig. 4). The value of α and β determined from the least square fitting of the formula to the data are estimates of, respectively, the initial HPC temperature and the undisturbed sediment temperature.

Unlike the oceanic heat flow probe discussed by Bullard (1954), the axial dissipation of heat by conduction through the conductive HPC may not be negligible. For the Bullard probe, the axial thermal constant of 18 days was large enough to confirm the adequacy of treating the problem of a 2.70-cm-diameter probe as two-dimensional radial thermal conduction. In the present case, the location of the temperature sensor in the core cutter near the lower end of the HPC indicates that axial heat flow by conduction will be more important. The corer's frictional heating is probably maximal in the shoe, or the lowermost part of the HPC, decreasing upward along the corer. If the conductive heat loss in the axial direction is nonnegligible, the actual cooling of the HPC must be faster than that given by the two-dimensional theory of thermal conduction, and the equilibrium sediment temperature will be reached within a shorter period of time. In this case, the value of β extrapolated theoretically from the cooling curve is a lower limit (T_{\min}) for the estimation of undisturbed sediment temperature.

On the other hand, the last undisturbed part of the cooling curve (D in Fig. 2) can be considered an upper limit (T_{\max}). The undisturbed sediment temperature lies between these bounds, probably closer to the lower. In the

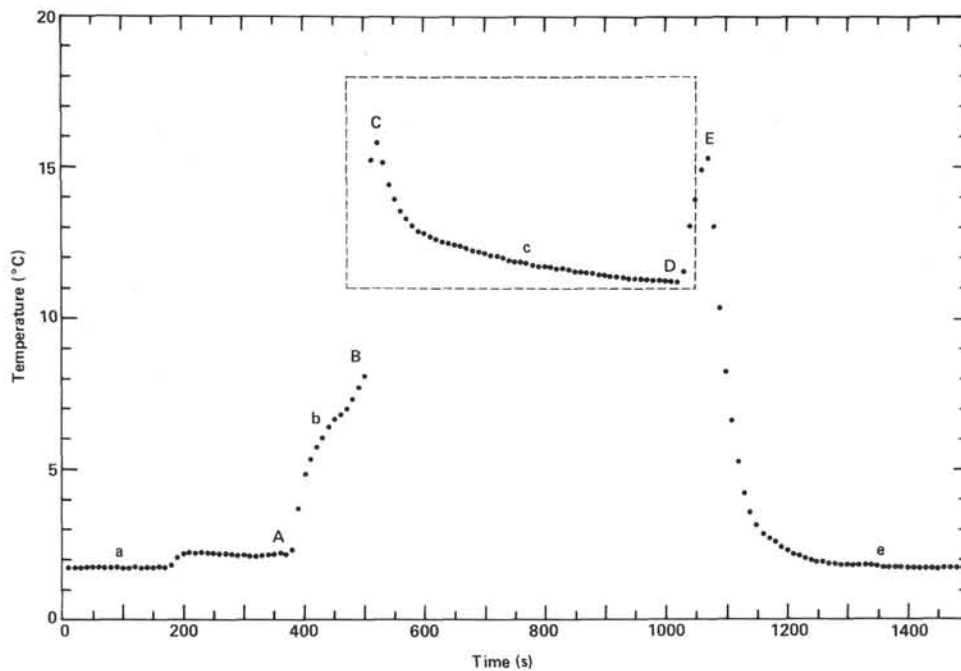


Figure 2. Example of temperature record taken with Core 578-14 at 128.3 m sub-bottom depth. The HPC is lowered into the drill pipe with a wire cable connected to a shipboard winch. By the time the corer approaches the seafloor, the temperature of the HPC is nearly equilibrated with the seawater temperature immediately above the seafloor (a). Upon entering the hole (A), the temperature rises, sensing an increasing temperature with depth (b). The corer is seated at the bottom of the drill pipe (B) and then thrust into the virgin sediment layer below the drilled hole by hydraulic pressure in the drill pipe controlled on the ship (C). The temperature rises rapidly, sensing the frictional heat generated at the contact surface of the corer with the sediment. The temperature then drops gradually as the corer remains stable and the frictional heat dissipates by conduction (c). The temperature of the HPC should eventually come to equilibrium with the surrounding sediment. The corer is retrieved (D), however, before the equilibrium temperature is reached. The temperature rises again, sensing the frictional heat of the extraction (E), and then subsides rapidly to the temperature of the bottom water (e) as the corer is raised.

following analysis of Leg 86 data, both bounds will be considered for each measurement whenever possible.

MEASUREMENT RESULTS

Site 576

The new temperature recording device was tested for the first time at Site 576. A total of 11 runs were made: 5 in Hole 576, 3 in Hole 576A, and 3 in Hole 576B. Seven runs were successful: 2 in Hole 576, 3 in Hole 576A, and 2 in Hole 576B. Run failures were due either to malfunctioning of the instrument or to mishandling in operation.

Even for the successful runs, the data quality was not as satisfactory as the example shown in Figure 2. In some of the data from Site 576, the frictional heating of the HPC at the time of probe penetration and extraction was not apparent, although the correction procedure of obtaining T_{\min} appears applicable to these data. For the data from Core 576-4, the duration of the HPC in the sediment was too short (<2 min) to apply any meaningful correction to the data. Therefore, only T_{\max} was read from the temperature record.

The results of temperature measurements at Site 576 are summarized in Table 1. The temperature at the sediment surface was estimated from the average of bottom

water temperatures recorded by the HPC prior to the hole entry. Figure 5 is a plot of T_{\max} and T_{\min} against sub-bottom sediment depth. The true undisturbed sediment temperature is believed to lie between T_{\max} and T_{\min} , probably closer to the latter in most cases.

Site 577

At Site 577, 15 runs were attempted (6 in Hole 577 and 9 in Hole 577A); 10 were successful (4 in Hole 577 and 6 in Hole 577A, Fig. 6). Generally, the quality of the temperature data was much improved over that recorded at Site 576. Based on the suggestion of the shipboard marine technicians, it was decided to release the tension in the cable suspending the HPC during operation of the heat flow instrument in the sediment. This appeared to eliminate transmission of much of the ship's motion to the HPC, which probably caused the small temperature fluctuations appearing in the otherwise smoothly varying cooling curves of the temperature record at Site 576.

For the data showing a monotonic gradual cooling, application of the correction procedure for obtaining T_{\min} by fitting a theoretical cooling curve to the measured temperature was straightforward. However, in the records obtained with Cores 577-8 (Fig. 7) and 577-12, a slight increase in temperature toward the end of the cooling

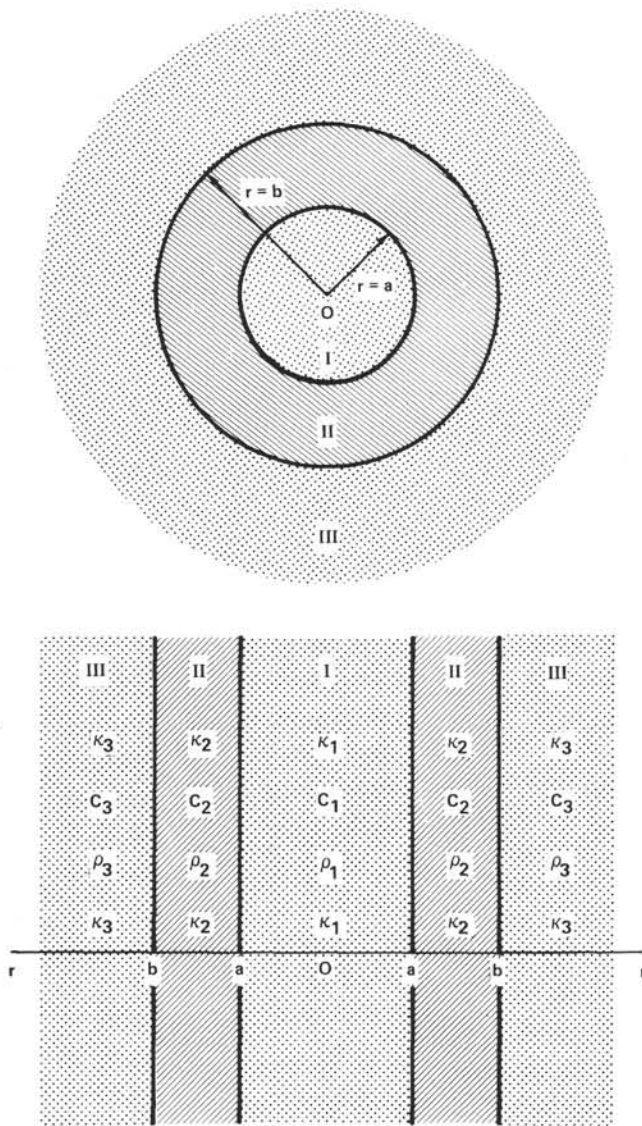


Figure 3. Composite circular cylinder model of the HPC embedded in the sediment. Upper section transverse to HPC axis, lower parallel.

curve was observed. The temperature record indicates the presence of a component that is increasing linearly with time, perhaps as a result of settling of the corer in the sediment. Accordingly, to describe the observed temperature, a term proportional to time, t , was added to the formula:

$$\alpha V(t) + \beta + \gamma t$$

The values of β obtained from the least-square fitting of the formula to the data are indicated as T_{\min} in parentheses in Table 1. The values of γ obtained by the same analysis were $0.211 \times 10^{-3} \text{C/s}$ for Core 577-8 and $0.582 \times 10^{-4} \text{C/s}$ for Core 577-12, that is, a total linear increase of temperature over the entire decay time in the bottom of 0.2 and 0.06°C , respectively.

As suggested above, the presence of the linear component in the data can be interpreted as indicating a

gradual sinking of the HPC in the sediment. The release of the cable tension during the operation of the heat flow instrument seems to favor this hypothesis. Assuming a linear vertical thermal gradient in the sediment of 0.04°C/m , the rates correspond to a respective sinking velocity of the HPC of 5.0 and 1.4 mm/s, respectively, not unreasonable for the heavy drill collars resting on a moderately soft sediment.

At the depth of Core 577A-8, the new HPC temperature recording device was operated with the conventional ERI-type temperature probe (Uyeda and Horai, 1981), the thermistor for the latter located about 20 cm below the HPC cutter tip. The sediment temperature measured by the ERI probe was 3.5°C higher than $T_{\max} = 4.39^\circ\text{C}$ recorded by the WHOI device. In the temperature record obtained by the latter, the HPC's temperature rises resulting from the frictional heating at core penetration and extraction were totally missing. The probe configuration is largely responsible for it. For the combined run, the ERI instrument was fixed inside the HPC with its temperature probe protruding from the shoe of the HPC. Therefore, the ERI probe should have made a better contact with the sediment. The run was made, however, without core sampling; that is, in the drilled section of the hole with the ERI probe contacting the unsampled sediment, while the contact of the HPC's shoe with the sediment might not have been complete. It is possible that both of the measured temperatures contain disturbances due to drilling that had not been removed completely. The result of temperature measurement made by the WHOI device, prior to the combined run, with the sampling of Core 577A-8 was $T_{\max} = 4.25$ and $T_{\min} = 4.19^\circ\text{C}$ (Table 1).

Site 578

One of the most successful series of heat flow measurements were made at Site 578 (Table 1). HPC temperature data taken at every two cores, or at an interval of 19 m, yielded an excellent profile for the range of sediment temperatures at the site. In Figure 8 are plotted T_{\max} and T_{\min} against the sub-bottom depth for Site 578.

For the data obtained with Core 578-2, the cooling curve was recorded for a relatively short period of time of 200 s. However, the data could still be fit satisfactorily to the theoretical cooling curve to obtain an estimate of T_{\min} with the least-square criterion. For other runs, the quality of data was generally satisfactory. Data collected with Cores 578-4 and 578-12 were, however, unsatisfactory because the HPC was mechanically unstable in the sediment as inferred from the discordant variation of the HPC temperature in the middle of cooling. The portion of the cooling curves before the disturbances was used to obtain an estimate of T_{\min} from the data. These different procedures may explain the anomalous gradient inferred between the measurements made on Cores 4 and 6 (Fig. 8).

Site 579

Bad weather prevented operation of the downhole temperature measurement for the first half of the drilling at

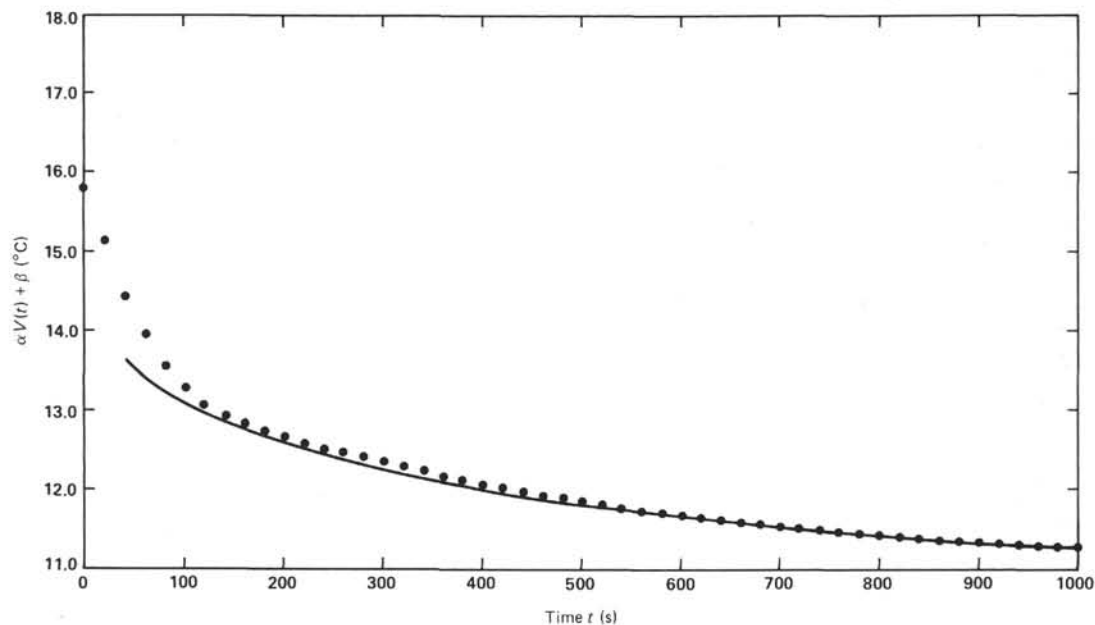


Figure 4. Fitting of theoretical formula $\alpha V(t) + \beta$ to the cooling HPC temperature of Figure 2 ($\alpha = 6.53^{\circ}\text{C}$, $\beta = 9.31^{\circ}\text{C}$).

Site 579. Better weather and moderated sea-surface conditions allowed the operation to resume at Core 9 and at every ensuing core to the bottom of the hole. All runs were successful (Table 1).

The temperature records were generally satisfactory. Only occasional breaks in the otherwise smooth-varying cooling curves suggest movement of the HPC corer in the drill pipe while the HPC was in the sediment. Undisturbed sediment temperatures could be estimated, however, from the portion of the cooling curves devoid of the breaks. The HPC's penetration into the sediment was incomplete with Core 579-15. Therefore, the validity of sediment temperature measured with that core is somewhat doubtful, even though the thermal decay was long and undisturbed.

A plot of T_{\max} and T_{\min} against the sub-bottom depths defines generally a linear increase of sediment temperature in the lower half of the drilled hole (Fig. 9).

Site 580

At Site 580, a total of 11 runs were attempted, all of which were successful (Table 1). Most of the recorded temperature data showed the HPC temperature smoothly decreasing with time after a rapid increase at the time of the HPC's penetration into the sediment. Therefore, estimates of T_{\max} and T_{\min} were not difficult to make. For the data obtained with Core 580-14, however, no significant variation of the temperature with time was observed to allow an estimation of T_{\min} . In Figure 10, the estimated sediment temperatures versus depth are plotted.

THERMAL CONDUCTIVITY RESULTS

Thermal conductivity was measured on 1056 soft sediment samples collected at Sites 576 to 580, in conjunction with the downhole temperature studies. A needle probe apparatus was used on board ship for measure-

ment of thermal conductivity. Detailed profiles of thermal conductivity versus depth through the soft sediment section recovered at each site are shown in Figures 11 to 15. The data were combined with the sediment temperature data to provide a value of heat flow (see below).

Calcite (CaCO_3) is among the rock-forming minerals that have the highest thermal conductivities. Accordingly, the thermal conductivity of the sediment increases with increasing calcium carbonate content if the sediment's water content is the same. At Site 577, the water depth (2675 m) is shallower than the Northwestern Pacific carbonate compensation depth of 3500–4000 m (Broecker and Takahashi, 1977). Probably, for this reason, Site 577 sediments have thermal conductivities that are generally higher than sediments from other sites of Leg 86 where the water depth exceeds the carbonate compensation depth.

The calcium carbonate content of the Site 577 sediments was determined on board ship on 38 selected samples from Hole 577 by the carbonate bomb method (see Site 577 chapter, this volume; Müller and Gastner, 1971). In Figure 16, on the plot of thermal conductivity versus porosity relationship, the calcium carbonate content of the sample is indicated by symbols. In order to show more clearly the increase of thermal conductivity with increasing calcium carbonate content, the range classification (Table 2) is compared (Fig. 17) with the grain thermal conductivity of the sample derived from the sample's water content by a formula adopted from Hashin and Shtrikman (Horai, 1981). The best fitting linear relationship indicates that the grain thermal conductivity of biogenic pelagic calcium carbonate is $4.5 \text{ W/m}\cdot\text{K}$.

HEAT FLOW RESULTS

From the sediment temperature data collected by the WHOI temperature recording device and the thermal conductivity data collected on board ship, heat flow was

Table 1. Results of temperature and thermal conductivity measurements at Sites 576, 577, 578, 579, and 580.

Core	Depth z (m)	Depth interval Δz (m)	Average thermal conductivity \bar{k} (W/m \cdot °K)	$\frac{\Delta z}{\bar{k}}$	$\Sigma \frac{\Delta z}{\bar{k}}$	Sediment temperature (°C)		
						T_w^a	T_{min}	T_{max}
Hole 576								
0	0 ^b							
4	31.2	31.2	0.754	41.39	41.39	1.59	—	5.38
6	50.2	19.0	0.756	25.13	66.52	1.58	5.38	6.29
Hole 576A								
2	18.2	18.2	0.743	24.50	24.50	—	3.21	3.54
4	37.2	19.0	0.806	23.57	48.07	1.66	4.65	5.56
7	65.7	28.5	0.970	29.38	77.45	1.65	5.89	6.41
Hole 576B								
6	55.7	55.7	0.821	67.84	67.84	1.66	(5.79)	5.99
7	65.2	9.5	1.061	8.95	76.80	1.67	6.05	6.70
Hole 577								
0	0							
4	35.3	35.3	0.979	36.06	36.06	1.73	(3.97)	4.66
6	54.3	19.0	1.062	17.89	53.95	1.77	4.04	5.47
8	73.3	19.0	1.199	15.85	69.80	1.82	(4.90)	(5.40)
12	111.3	38.0	1.238	30.695	100.49	1.77	(6.23)	6.87
Hole 577A								
4	37.9	37.9	1.040	36.44	36.44	1.74	(3.39)	4.63
6	56.9	19.0	1.095	17.35	53.79	1.78	(3.70)	5.91
8	75.9	19.0	1.138	16.70	70.49	1.76	4.19	4.25
10	94.9	19.0	1.267	15.00	85.49	1.79	5.73	6.29
12	113.9	19.0	1.165	16.31	101.80	1.85	(6.38)	7.28
Hole 578								
0	0							
2	14.3	14.3	0.745	19.20	19.20	1.69	(3.15)	3.46
4	33.3	19.0	0.777	24.45	43.65	1.68	(4.53)	4.95
6	52.3	19.0	0.722	26.32	69.96	1.66	4.79	6.37
8	71.3	19.0	0.778	24.42	94.39	1.65	6.00	7.79
10	90.3	19.0	0.791	24.02	118.41	1.76	7.09	7.74
12	109.3	19.0	0.766	23.43	143.21	1.73	(8.06)	9.64
14	128.3	19.0	0.811	23.43	166.64	1.77	9.31	11.24
Hole 579								
0	0							
9	99.5	99.5	0.733	135.74	135.74	1.70	7.76	9.05
10	109.0	9.5	0.696	13.65	149.39	1.74	8.96	9.67
11	118.5	9.5	0.695	13.67	163.06	1.78	9.18	10.29
12	128.0	9.5	0.690	13.77	176.83	1.76	9.65	11.10
13	137.5	9.5	0.669	14.20	191.03	1.82	9.99	11.75
14	147.0	9.5	0.710	13.38	204.41	1.83	11.30	12.43
15	156.5	9.5	0.730	13.01	217.43	1.82	(11.08)	(11.89)
Hole 580								
0	0							
3	22.3	22.3	0.754	29.58	29.58	1.60	3.08	3.29
5	41.3	19.0	0.792	23.99	53.57	1.66	4.13	4.30
		19.0	0.736	25.82				

Table 1. (Continued).

Core	Depth z (m)	Depth interval Δz (m)	Average thermal conductivity \bar{k} (W/m \cdot °K)	$\frac{\Delta z}{\bar{k}}$	$\Sigma \frac{\Delta z}{\bar{k}}$	Sediment temperature (°C)		
						T_w^a	T_{min}	T_{max}
Hole 580 (Continued)								
7	60.3	9.5	0.795	11.95	79.38	1.63	5.21	5.66
8	69.8	9.5	0.776	12.24	91.33	1.65	5.73	6.93
9	79.3	9.5	0.803	11.83	103.57	1.62	6.54	7.32
10	88.8	9.5	0.780	12.18	115.40	1.59	6.80	7.51
11	98.3	19.0	0.779	24.39	127.58	1.65	7.16	8.43
13	117.3	9.5	0.869	10.93	151.97	1.71	8.39	9.26
14	126.8	9.5	0.859	11.06	162.91	1.71	—	9.88
15	136.3	19.0	0.785	24.20	173.96	1.68	9.55	10.61
17	155.3				198.17	1.71	10.51	11.85

^a Bottom water temperature recorded by the HPC prior to the hole entry.
^b Sediment surface temperature estimated as an average of T_w is 1.64°C at Site 576, 1.78°C at Site 577, 1.71°C at Site 578, 1.78°C at Site 579, and 1.65°C at Site 580. Data points of questionable quality are in parentheses. — indicates lack of appropriate data to estimate T_{min} .

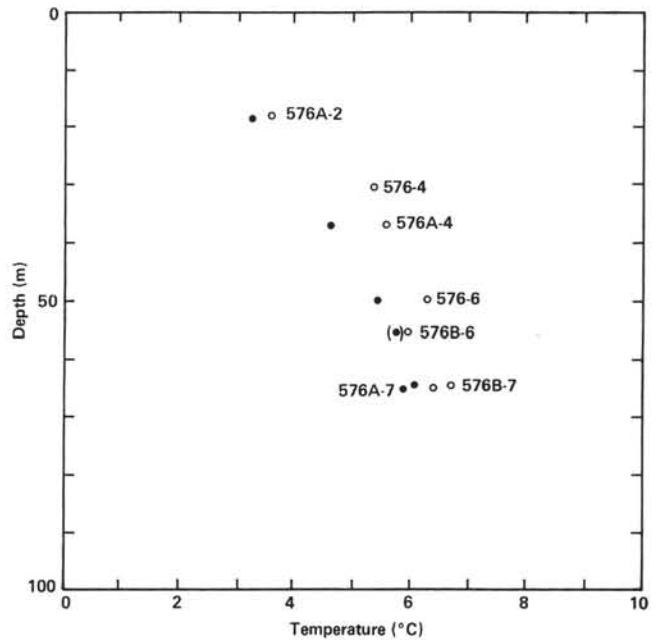


Figure 5. Results of sediment temperature measurements at Site 576. Open circles for T_{max} ; filled circles for T_{min} . Data points of questionable quality are in parentheses.

obtained by the method of Bullard (1939). In the sub-bottom depth interval from z_0 to z , sediment temperature $T(z)$ is related to thermal conductivity $k(z)$ as

$$T(z) = T_0 + Q \int_{z_0}^z k(z)^{-1} dz$$

where T_0 is the temperature at the depth z_0 and Q is the steady-state conducted heat flow. If the measured sediment temperature $T_i = T(z_i)$, $i = 1, 2, \dots, n$ is plotted against the cumulative thermal resistance

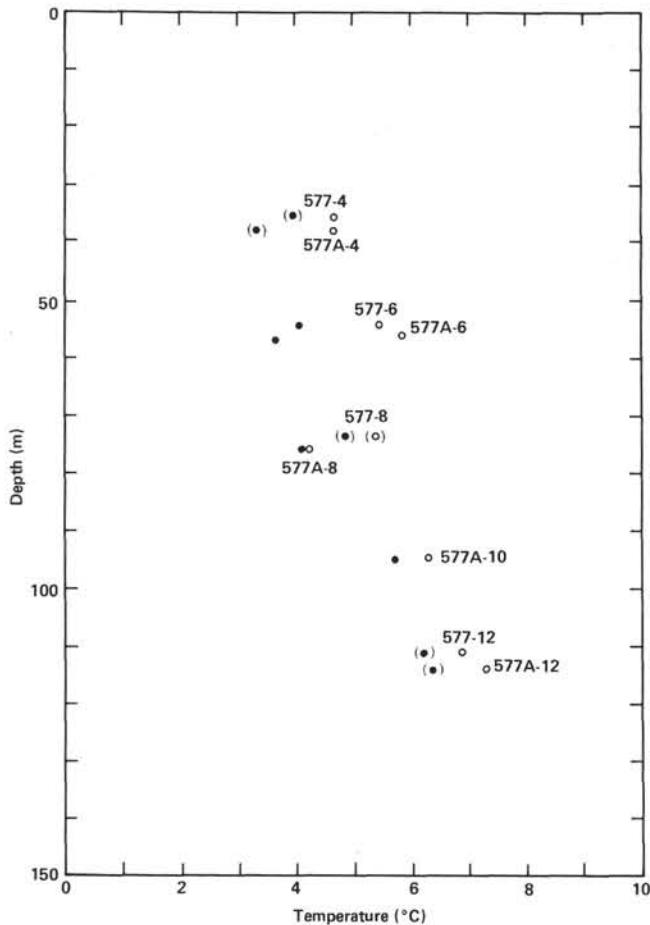


Figure 6. Results of sediment temperature measurements at Site 577. Data points of questionable quality are in parentheses. For symbols, see caption of Figure 5.

$$R_i = \sum_{j=1}^i \Delta z_j / \bar{k}_j, \quad i = 1, 2, \dots, n,$$

then the slope will give an estimate of Q . A geometric mean of the measured sample thermal conductivities in the depth interval $\Delta z_j = z_j - z_{j-1}$ was used for an estimate of

$$\bar{k}_j^{-1} = \int_{z_{j-1}}^z k(z)^{-1} dz.$$

Upper and lower bounds of heat flow, Q_{\max} and Q_{\min} , were calculated from the bounds of sediment temperature, T_{\max} and T_{\min} , for each site.

Site 576

The concave downward temperature distribution (Fig. 5) observed at Site 576 may indicate a decrease of thermal gradient with depth, and/or the presence of hydrothermal circulation in the sediment on young crust (Anderson and Skilbeck, 1981). At the present site, however, the change of thermal gradient is largely accounted for by the distribution of thermal conductivity, which is markedly different above and below a sub-bottom depth of 55 m (Fig. 11). A plot of sediment temperature against the cumulative thermal resistivity showed a more uniform distribution of heat flow, $Q_{\max} = 61.2 \text{ mW/m}^2$ and $Q_{\min} = 56.0 \text{ mW/m}^2$ (Fig. 18). A more detailed and accurate measurement of sediment temperature is necessary to confirm any convective motion of water in the sediment.

Site 577

The temperature reversal apparent in the plot of T_{\max} against the cumulative thermal resistance is less conspic-

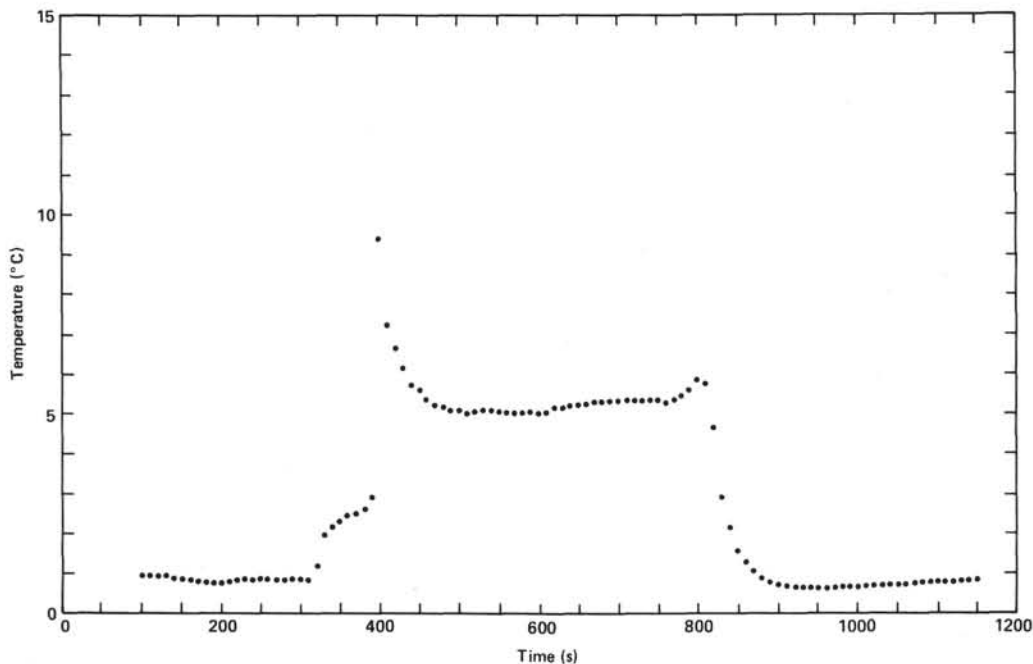


Figure 7. Temperature record taken with Core 577-8 (sub-bottom depth 73.3 m).

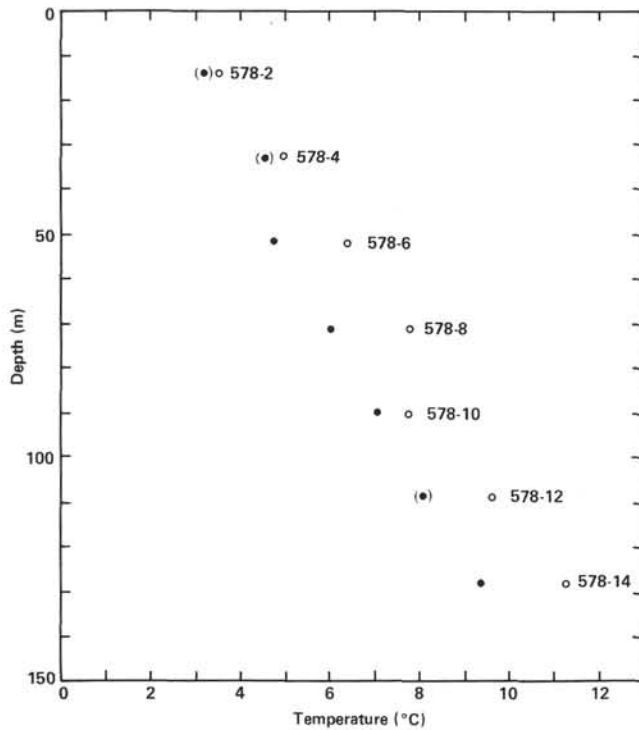


Figure 8. Results of sediment temperature measurements at Site 578. For symbols, see caption of Figure 5.

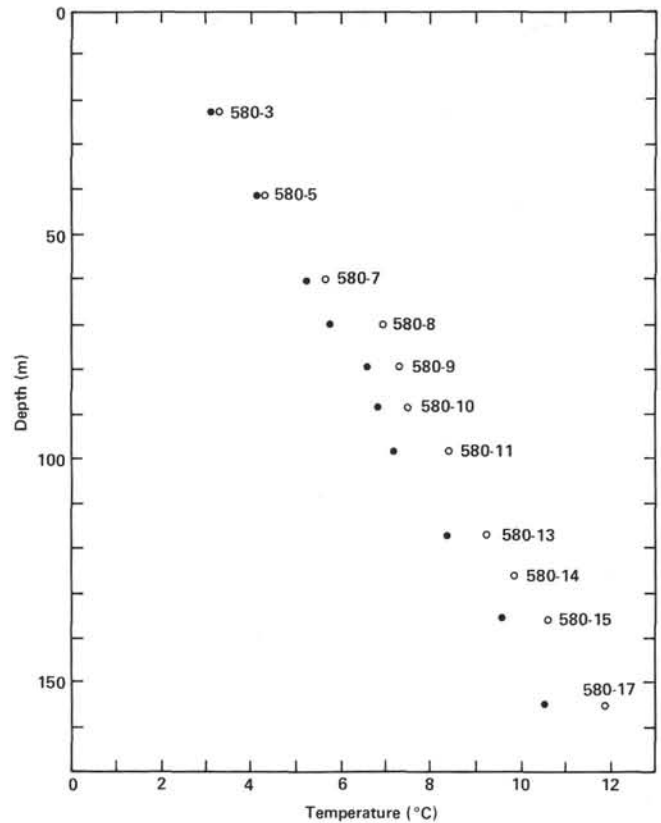


Figure 10. Results of sediment temperature measurements at Site 580. For symbols, see caption of Figure 5.

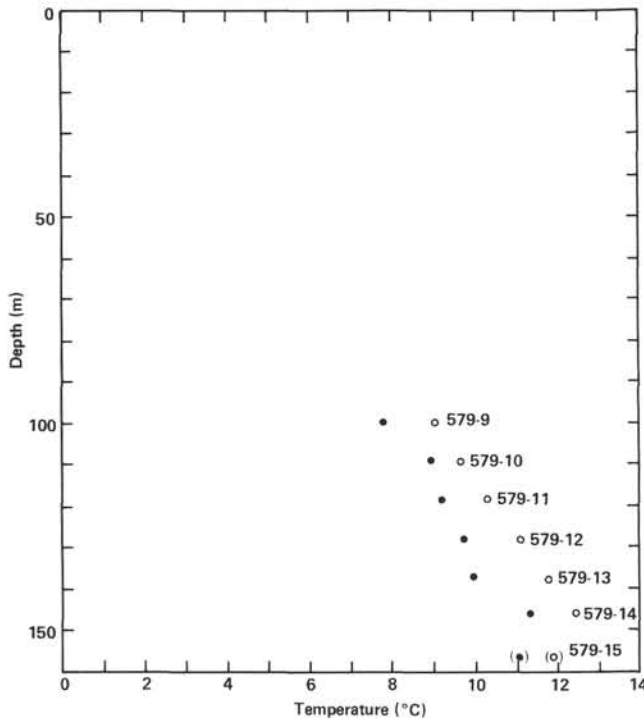


Figure 9. Results of sediment temperature measurements at Site 579. For symbols, see caption of Figure 5.

uous in the plot of T_{min} (Fig. 19). A straight line fit to the data gave $Q_{max} = 44.1 \text{ mW/m}^2$ and $Q_{min} = 39.2 \text{ mW/m}^2$. This will not be very far from the range of present heat flow at Site 577.

Site 578

$Q_{max} = 52.9 \text{ mW/m}^2$ and $Q_{min} = 42.7 \text{ mW/m}^2$ are indicated by the temperature versus cumulative thermal resistivity plot (Fig. 20).

Site 579

A constant heat flow of $Q_{max} = 49.7 \text{ mW/m}^2$ and $Q_{min} = 44.1 \text{ mW/m}^2$ is indicated from the data (Fig. 21). This is only representative, however, of the lower section of the drilled hole, from the depth of 120 to 220 m sub-bottom.

Site 580

The data (Fig. 22) indicate $Q_{max} = 51.4$ and $Q_{min} = 44.4 \text{ mW/m}^2$ that are almost uniform over the entire length of the hole to a sub-bottom depth of 200 m.

Table 3 is a summary of heat flow results. The lithospheric ages of the sites determined from Mesozoic magnetic lineations of the Northwestern Pacific were taken from Hilde et al. (1976). Figure 23 summarizes the heat flow results at the different sites. A plot of the heat flow range versus lithospheric age in Figure 24 agrees, within the range of data uncertainty, with the average heat flow versus age relationship in the North Pacific (Sclater et al., 1980) and with recent field work designed to test that relationship (J. Sclater, personal communication, 1984). Probably, the lithospheric thermal structure under DSDP Leg 86 sites is not very far from that deduced

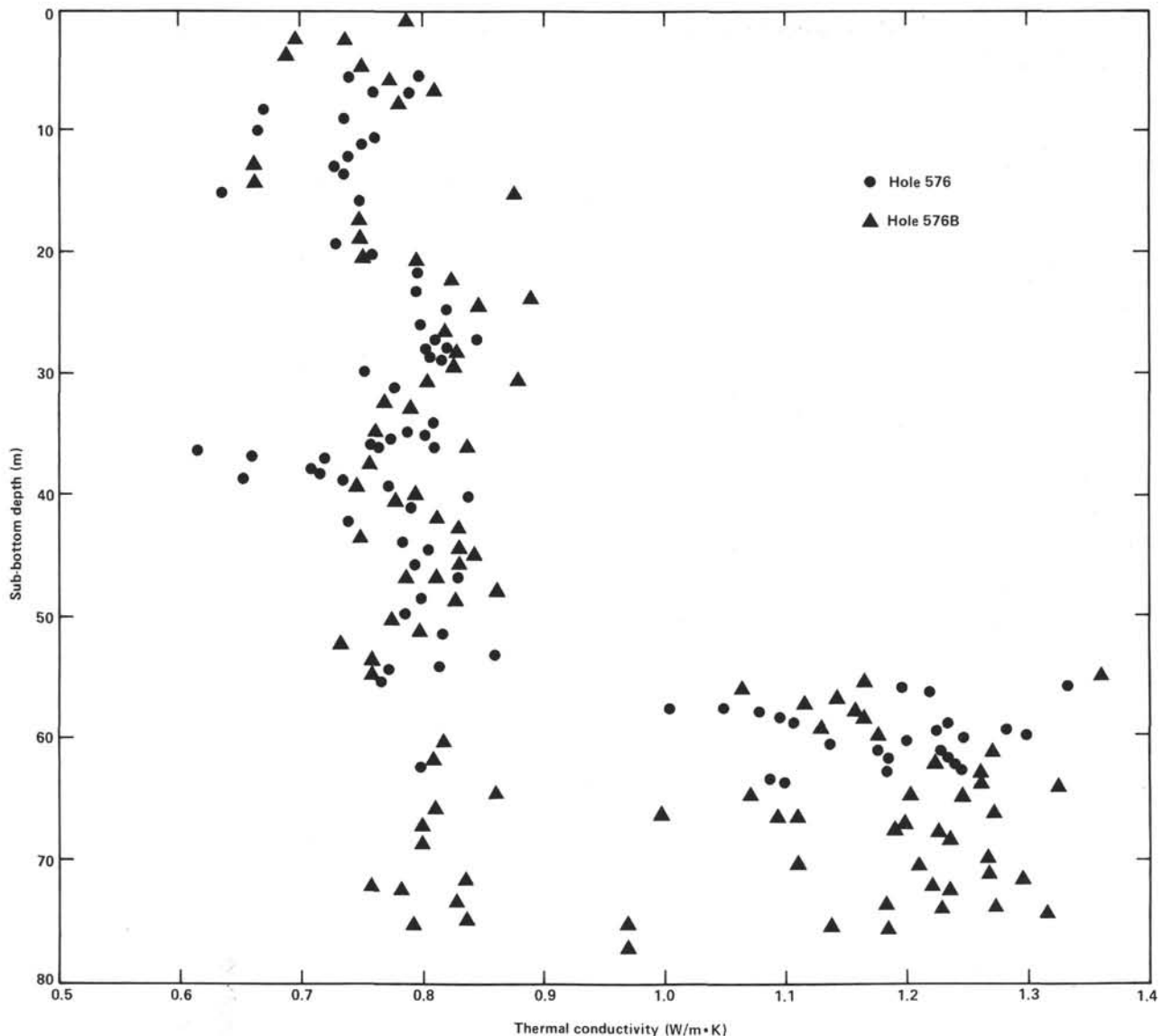


Figure 11. Sediment thermal conductivity versus sub-bottom depth at Site 576.

by the thermal boundary layer model (Parsons and McKenzie, 1978).

CONCLUSION

The new temperature recording device recently designed and constructed at Woods Hole Oceanographic Institution proved useful in recording the temperature measured in DSDP drill holes during Leg 86. The measured temperature data were used to estimate the possible range of undisturbed sediment temperature. These data were then combined with the thermal conductivity of sediment samples for calculation of heat flow. We expect to refine the theory of correcting the temperature data for the disturbance caused by the drilling to improve the estimation of undisturbed sediment temperature.

In general, where the quality of data is good, the new technique of downhole temperature measurements in conjunction with HPC operations demonstrated linear conductive temperature gradients (Sites 578 and 580) as ex-

pected for these old well-sedimented sites in the western Pacific. However, even when the measurements are disturbed or otherwise not as satisfactory (Sites 577 and 579), the ability to obtain relatively numerous measurements during coring operations allowed estimation of gradients with relatively small uncertainties (Table 3). The method appears to be capable of providing significantly improved heat flow estimates during HPC operations, with much less time than previously used techniques (Erickson, 1973; Yokota et al., 1980).

ACKNOWLEDGMENTS

This paper was improved by the helpful reviews of V. Vacquier and E. Davis. The development of instrumentation was supported initially by the U.S. Geological Survey (Marine Geology) at Woods Hole, the Ocean Industry Program of the Woods Hole Oceanographic Institution, and DSDP; subsequent funding was from U.S. National Science Foundation Grants OCE82-14658 and 83-00073. We are grateful to the officers, crew, and technical staff aboard the *Glomar Challenger* whose skills and assistance made these measurements possible.

REFERENCES

- Anderson, R. N., and Skilbeck, J. N., 1981. Oceanic heat flow. In Emiliani, C. (Ed.), *The Sea* (Vol. 7): New York (Wiley-Interscience), 489-523.
- Broecker, W. S., and Takahashi, T., 1977. The solubility of calcite in sea water. In Frazer, D. Z. (Ed.), *Thermodynamics in Geology*: Dordrecht (D. Reidel), pp. 365-379.
- Bullard, E. C., 1939. Heat flow in South Africa. *Proc. R. Soc. London, Ser. A*, 173:474-502.
- Burns, R. E., 1970. Heat flow operations at Holes 35.0 and 35.1 In McManus, D. A., Burns, R. E., et al., *Init. Repts. DSDP*, 5: Washington (U.S. Govt. Printing Office), 551-554.
- Erickson, A., 1973. Initial report on downhole temperature and shipboard thermal conductivity measurements, Leg 19, Deep Sea Drilling Project. In Creager, J. S., Scholl, D. W., et al., *Init. Repts. DSDP*, 19: Washington (U.S. Govt. Printing Office), 643-656.
- Erickson, J. A., and Hyndman, R. D., 1979. Downhole temperature measurements and thermal conductivities of samples, Site 396 Deep Sea Drilling Project Leg 46. In Dmitriev, L., Heirtzler, J., et al., *Init. Repts. DSDP*, 46: Washington (U.S. Govt. Printing Office), 389-400.
- Girdler, R. W., Erickson, A. J., and Von Herzen, R. P., 1974. Downhole temperature and shipboard thermal conductivity measurements aboard D/V *Glomar Challenger* in the Red Sea. In Whitmarsh, R. B., Weser, O. E., Ross, D. A., et al., *Init. Repts. DSDP*, 23: Washington (U.S. Govt. Printing Office), 879-886.
- Hilde, T. W. C., Isezaki, N., and Wageman, J. M., 1975. Mesozoic sea-floor spreading in the North-Pacific. In Sutton, G. H., Manghnan, M. H., and Moberly, R. (Eds.), *The Geophysics of the Pacific Ocean Basin and Its Margin*: Washington (American Geophysical Union), pp. 205-226.
- Horai, K., 1981. Thermal conductivity of sediments and igneous rocks recovered during Deep Sea Drilling Project Leg 60. In Hussong, D. M., Uyeda, S., et al., *Init. Repts. DSDP*, 60: Washington (U.S. Govt. Printing Office), 807-834.
- Hyndman, R. D., Erickson, A. J., and Von Herzen, R. P., 1974. Geothermal measurements on DSDP Leg 26. In Davies, T. A., Luyendyk, B. P., et al., *Init. Repts. DSDP*, 26: Washington (U.S. Govt. Printing Office), 451-464.
- Hyndman, R. D., Von Herzen, R. P., Erickson, A. J., and Jolivet, J., 1977. Heat flow measurements, DSDP Leg 37. In Aumento, F., Melson, W. G., et al., *Init. Repts. DSDP*, 37: Washington (U.S. Govt. Printing Office), 347-362.
- Marshall, B. V., and Erickson, A. J., 1974. Heat flow and thermal conductivity measurements, Leg 25, Deep Sea Drilling Project. In Simpson, E. S. W., Schlich, R., et al., *Init. Repts. DSDP*, 25: Washington (U.S. Govt. Printing Office), 349-355.
- Müller, G., and Gastner, M., 1971. The "Karbonat Bombe", a simple device for determination of the carbonate content in sediments, soils, and other materials. *Neues. Jahrb. Mineral. Monatsh.*, 10: 466-469.
- Parsons, B., and McKenzie, D. P., 1978. Mantle convection and the thermal structure of the plates. *J. Geophys. Res.*, 83:4485-4496.
- Slater, J. G., and Erickson, A. J., 1974. Geothermal measurements on Leg 22 of the D/V *Glomar Challenger*. In von der Borch, C. C., Slater, J. G., et al., *Init. Repts. DSDP*, 22: Washington (U.S. Govt. Printing Office), 387-396.
- Slater, J. G., Jaupart, C., and Galson, D., 1980. The heat flow through oceanic and continental crust and the heat loss of the earth. *Rev. Geophys. Space Phys.*, 18:269-311.
- Uyeda, S., and Horai, K., 1982. Heat flow measurements on Deep Sea Drilling Project Leg 60. In Hussong, D. M., Uyeda, S., et al., *Init. Repts. DSDP*, 60: Washington (U.S. Govt. Printing Office), 789-800.
- Von Herzen, R. P., 1973. Geothermal measurements, Leg 21. In Burns, R. E., Andrews, J. E., et al., *Init. Repts. DSDP*, 21: Washington (U.S. Govt. Printing Office), 443-458.
- Von Herzen, R. P., Fiske, R. J., and Sutton, G., 1971. Geothermal measurements on Leg 8. In Tracey, J. I., Jr., Sutton, G. H., et al., *Init. Repts. DSDP*, 8: Washington (U.S. Govt. Printing Office), 837-849.
- Watanabe, T., Von Herzen, R. P., and Erickson, A. J., 1975. Geothermal studies Leg 31, Deep Sea Drilling Project. In Karig, D. E., Ingle, J. C., Jr., et al., *Init. Repts. DSDP*, 31: Washington (U.S. Govt. Printing Office), 573-576.
- Yokota, T., Kinoshita, H., and Uyeda, S., 1980. New DSDP (Deep Sea Drilling Project) downhole temperature probe utilizing IC RAM (Memory) elements. *Bull. Earthquake Res. Inst., Univ. Tokyo*, 55: 75-88.

Date of Initial Receipt: 19 March 1984

Date of Acceptance: 2 October 1984

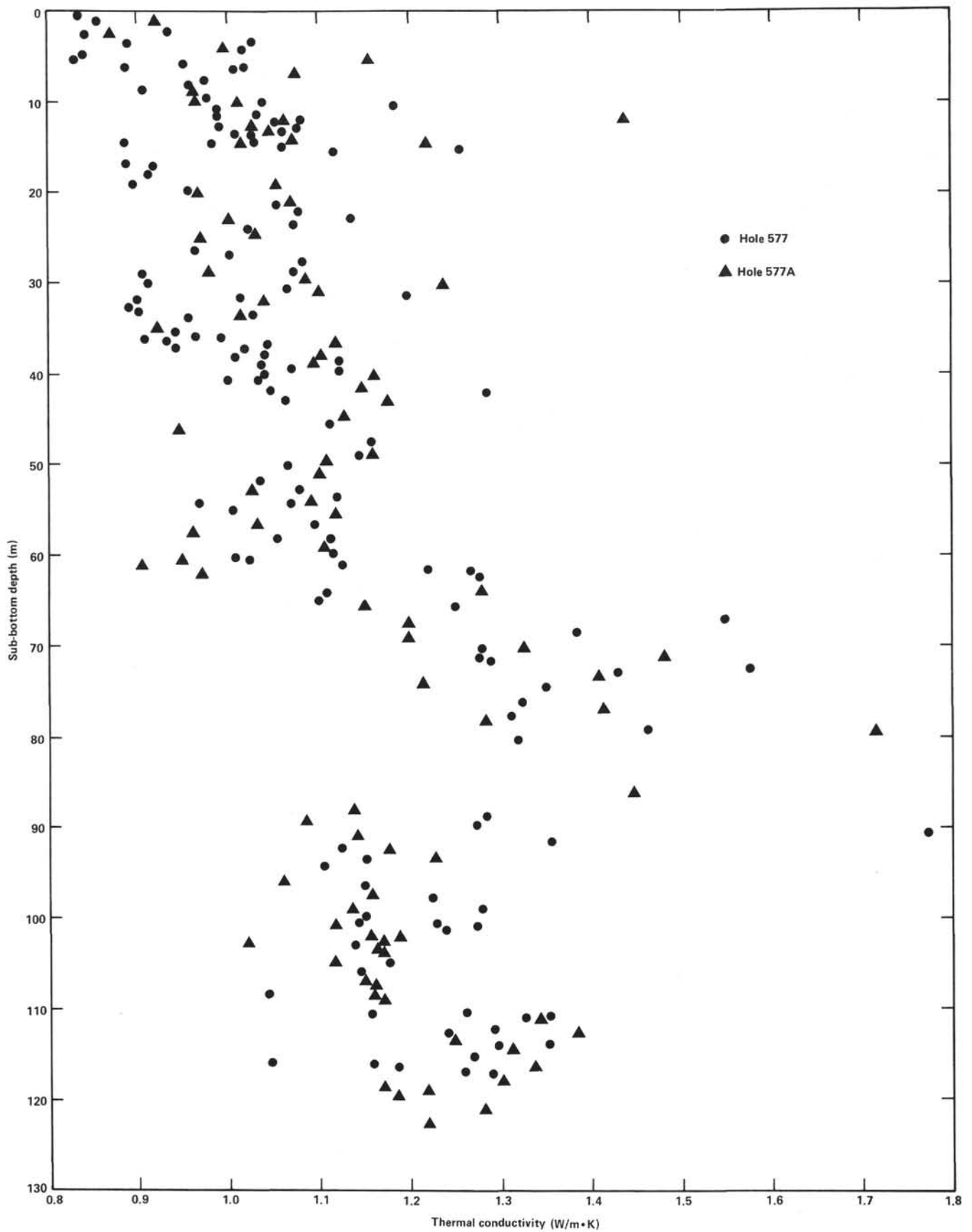


Figure 12. Sediment thermal conductivity versus sub-bottom depth at Site 577.

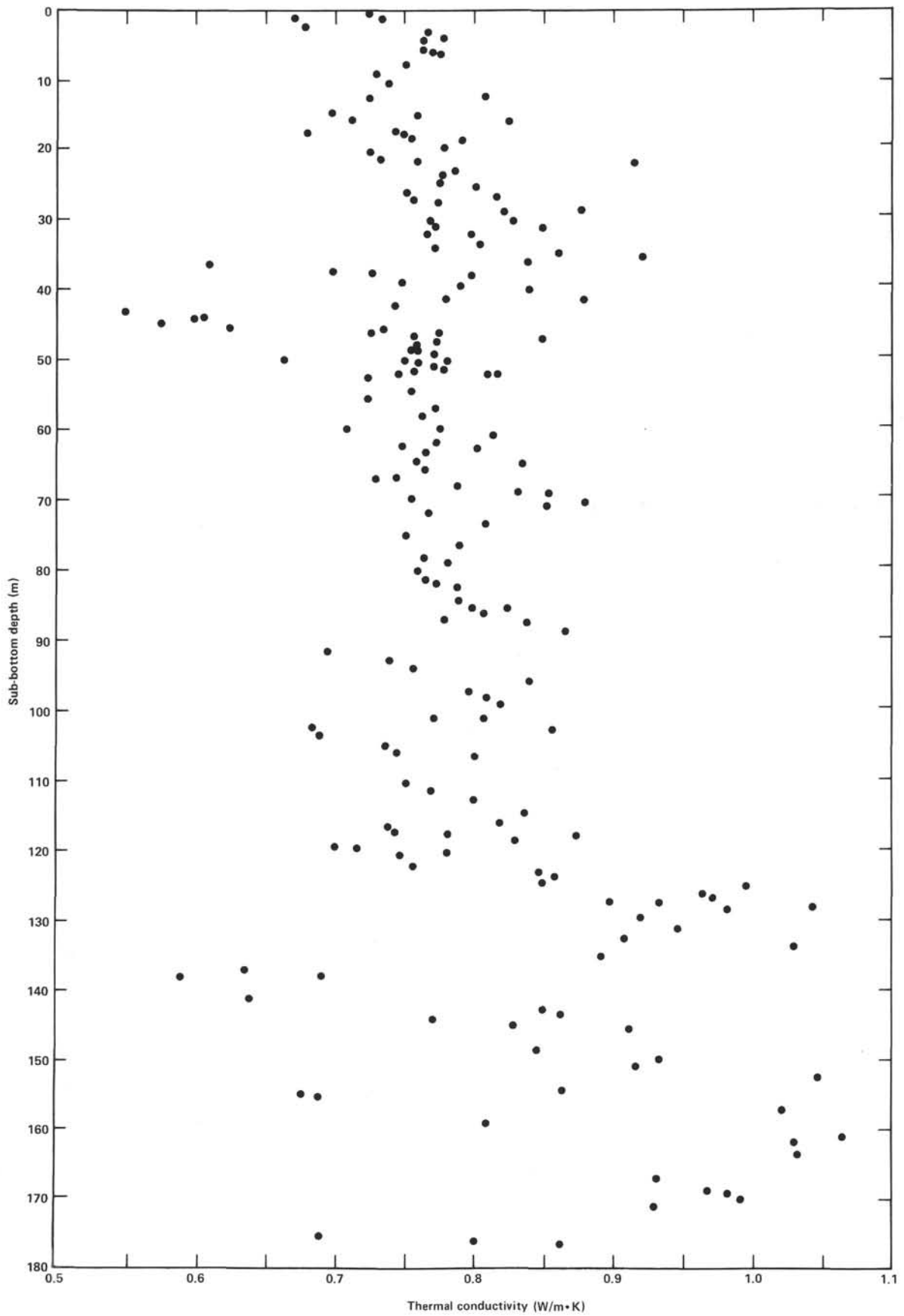


Figure 13. Sediment thermal conductivity versus sub-bottom depth at Site 578.

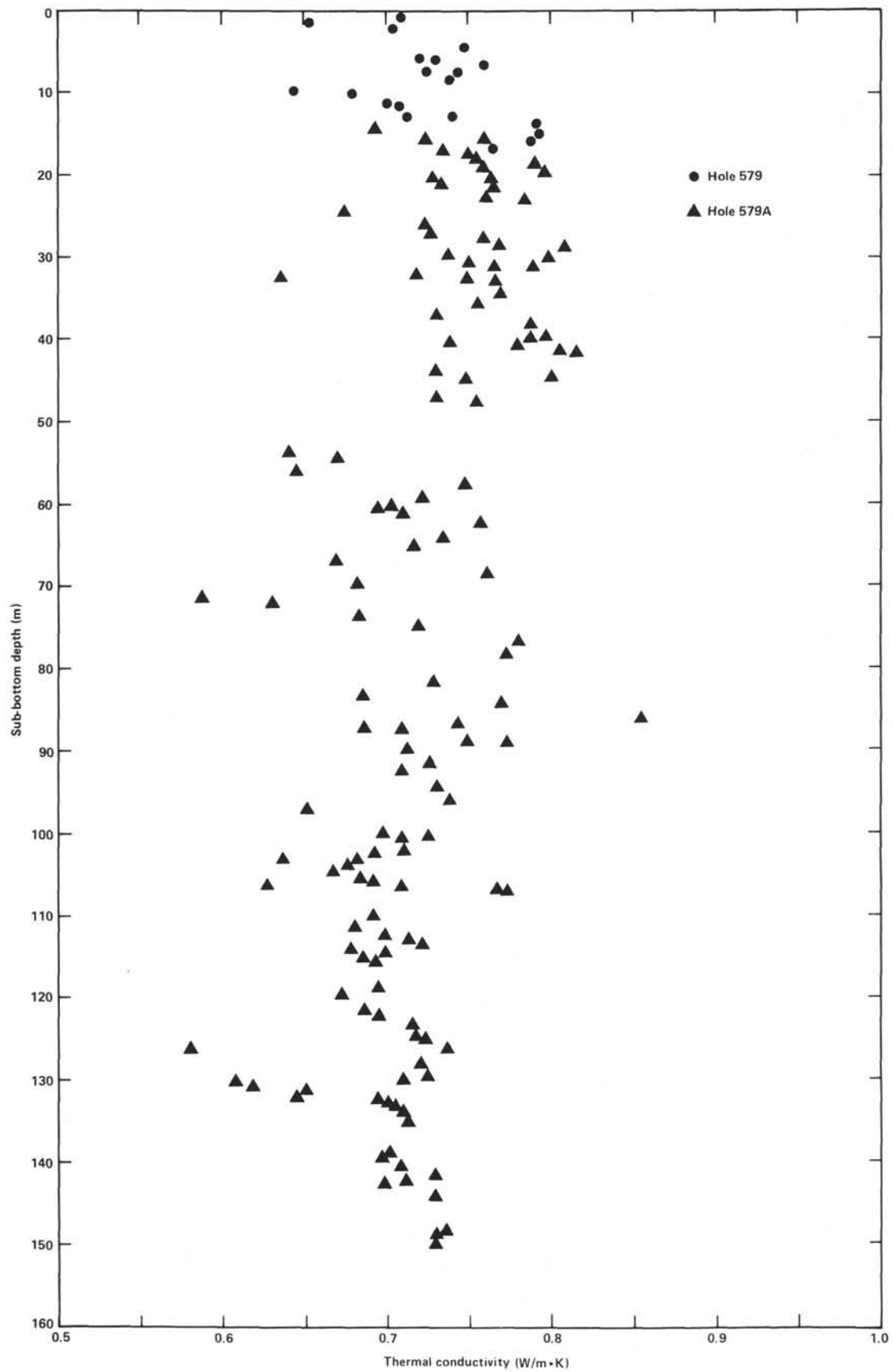


Figure 14. Sediment thermal conductivity versus sub-bottom depth at Site 579.

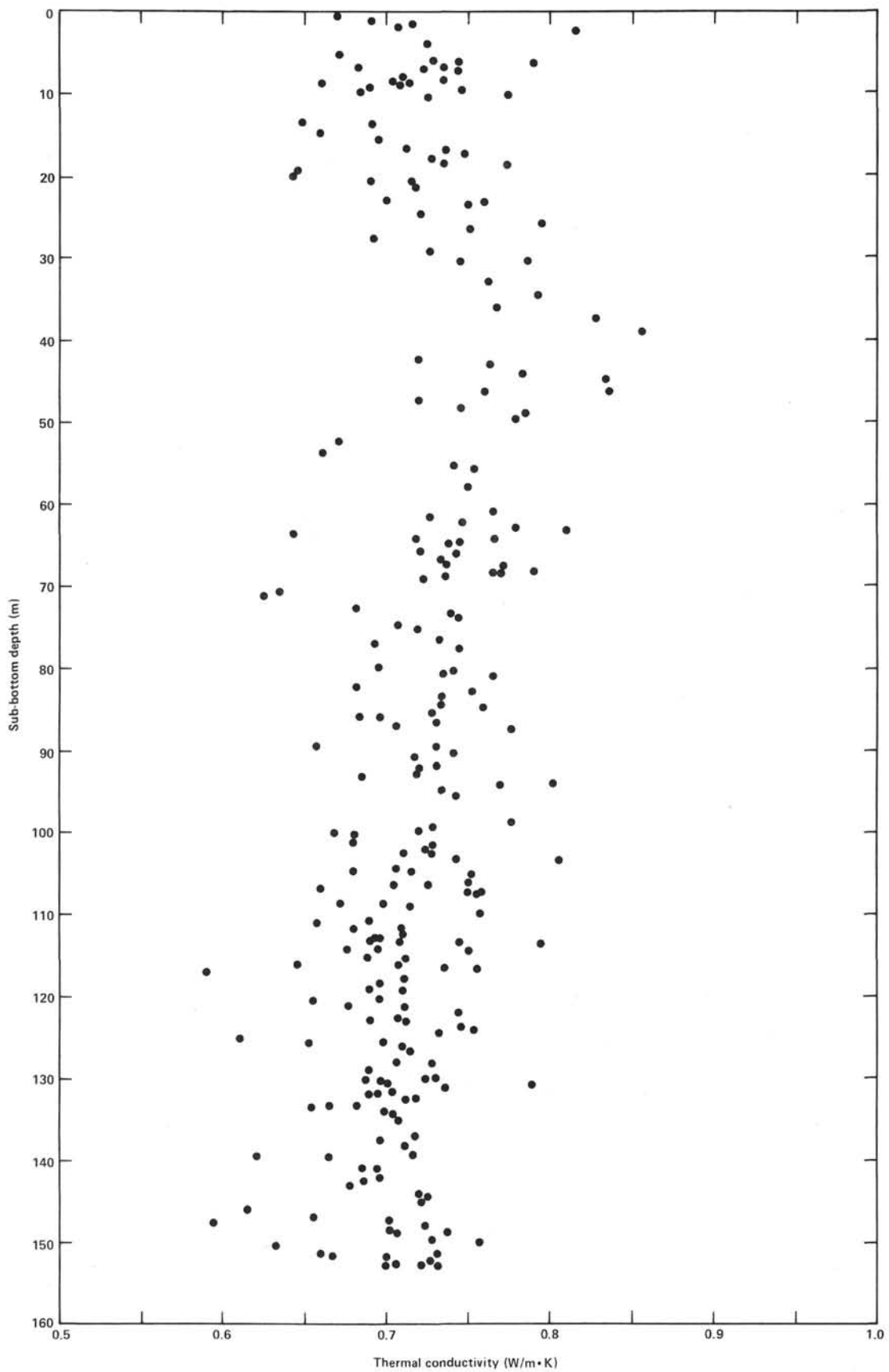


Figure 15. Sediment thermal conductivity versus sub-bottom depth at Site 580.

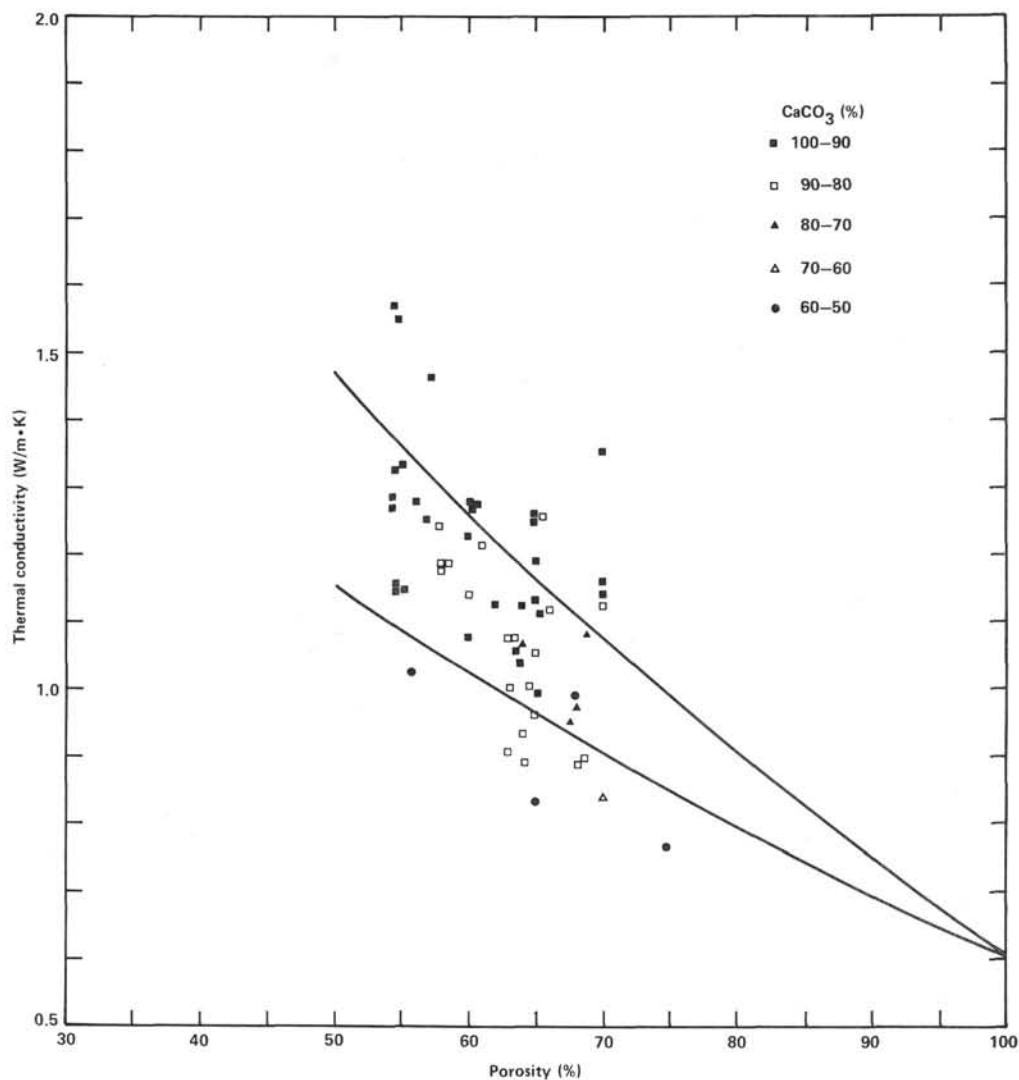


Figure 16. Sediment thermal conductivity versus porosity relationship for various calcium carbonate (CaCO_3) contents.

Table 2. Calcium carbonate content and thermal conductivity of Site 577 sediment samples, Leg 86.

Range of CaCO_3 content by weight (%)	Thermal conductivity $k + \Delta k$ (s.d.) ($\text{W}/\text{m}\cdot\text{K}$)	Sample size
90-100	4.37 ± 0.63	12
80-90	3.84 ± 0.54	18
70-80	4.30 ± 0.70	3
60-70	3.70 ± 0.50	2
50-60	3.21 ± 0.84	3

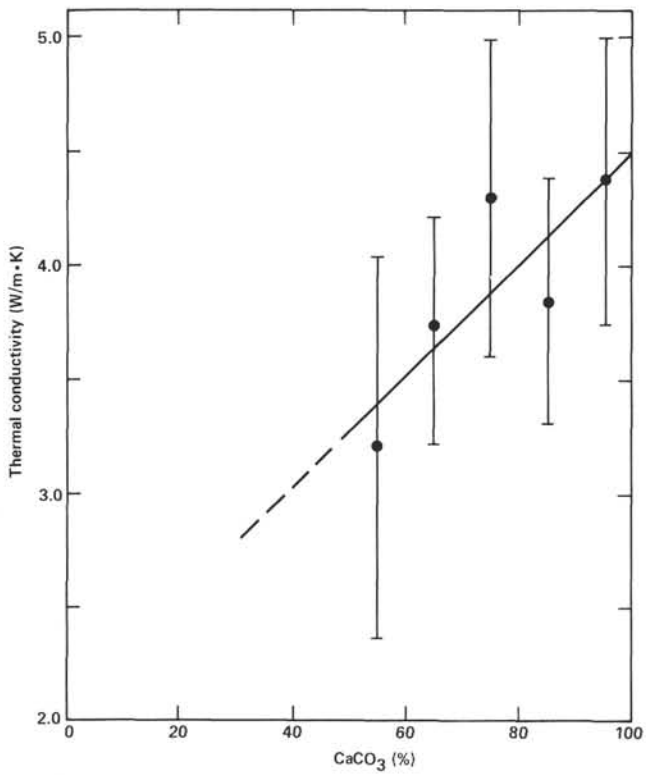


Figure 17. Grain thermal conductivity of sediment as a function of calcium carbonate content by weight.

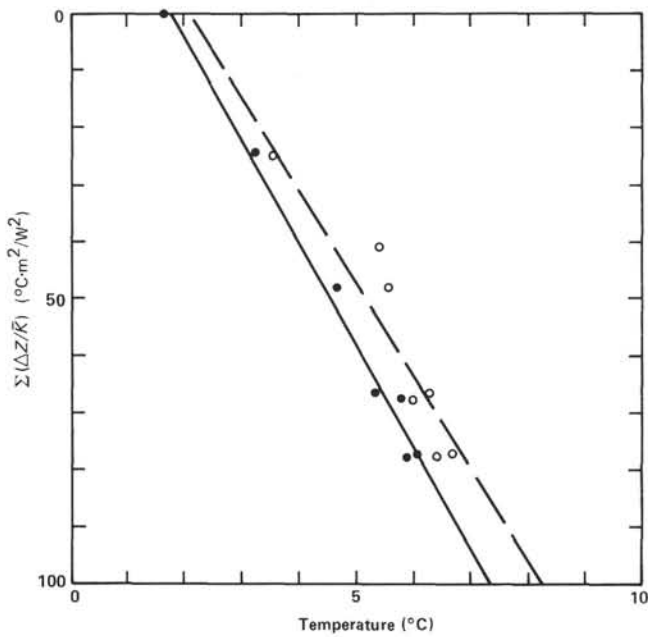


Figure 18. Plot of sediment temperatures, T_{max} and T_{min} , against cumulative thermal resistance at Site 576.

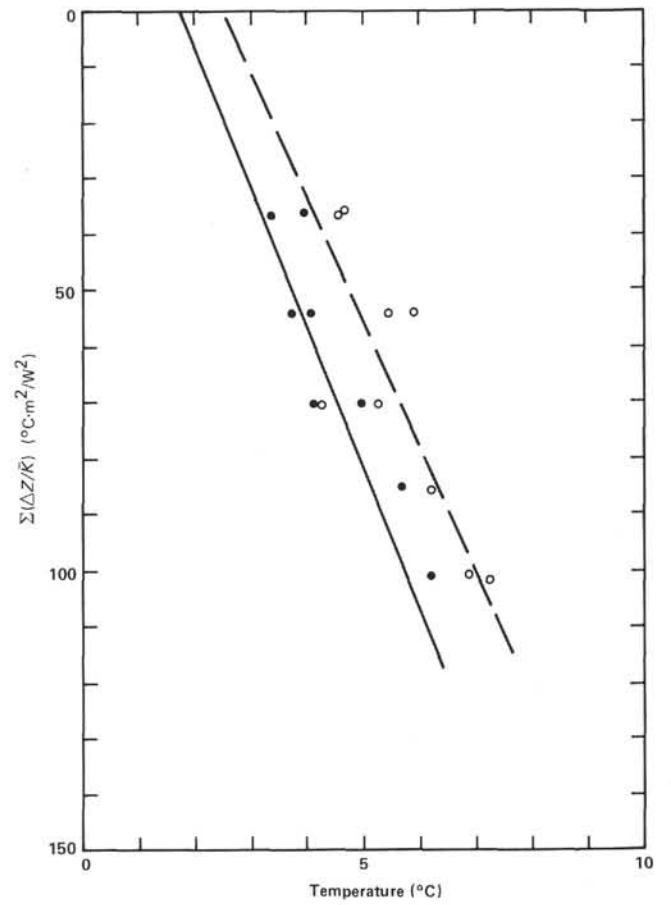


Figure 19. Plot of sediment temperatures, T_{max} and T_{min} , against cumulative thermal resistance at Site 577.

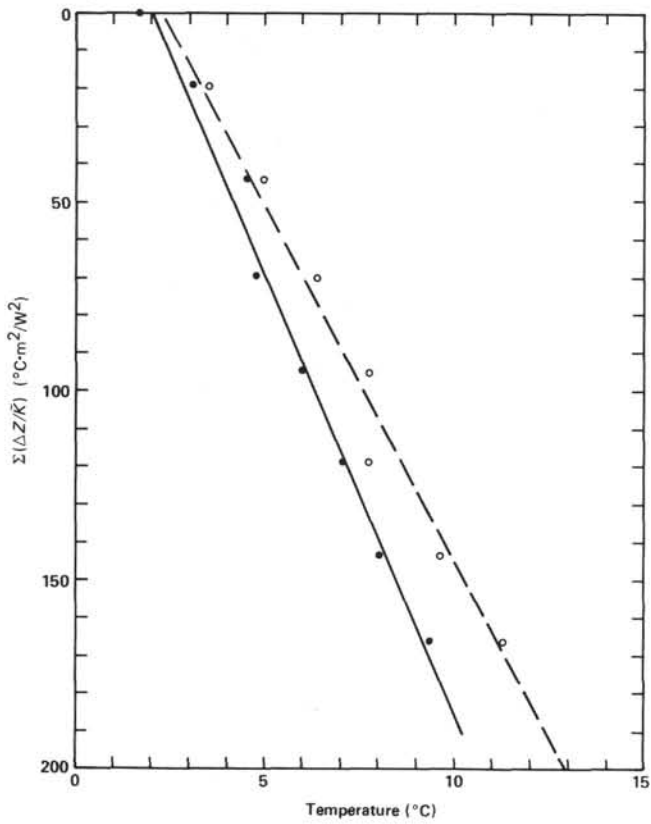


Figure 20. Plot of sediment temperatures, T_{\max} and T_{\min} , against cumulative thermal resistance at Site 578.

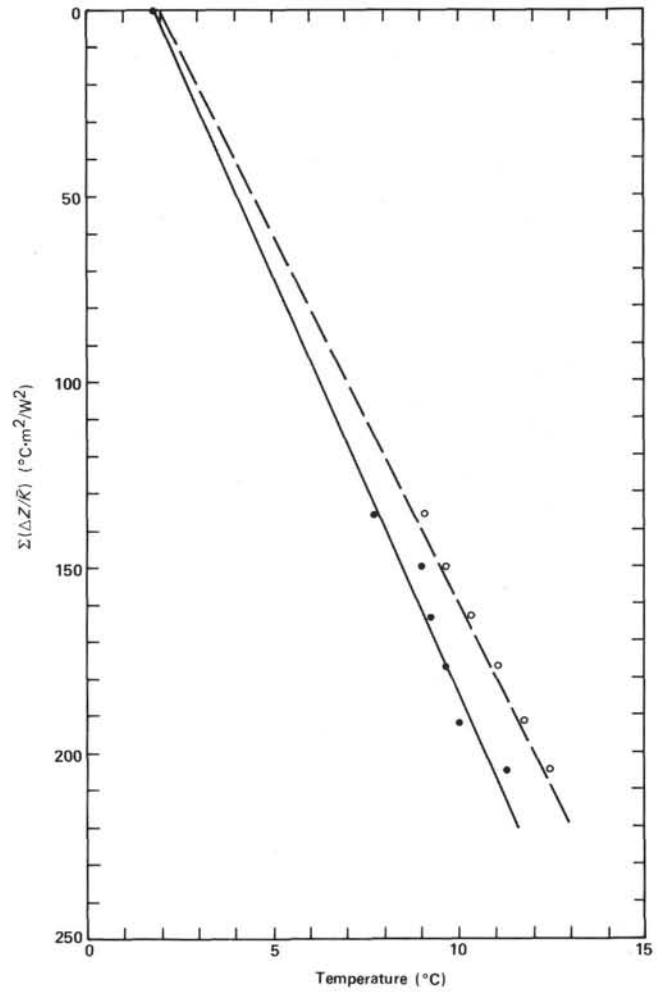


Figure 21. Plot of sediment temperatures, T_{\max} and T_{\min} , against cumulative thermal resistance at Site 579.

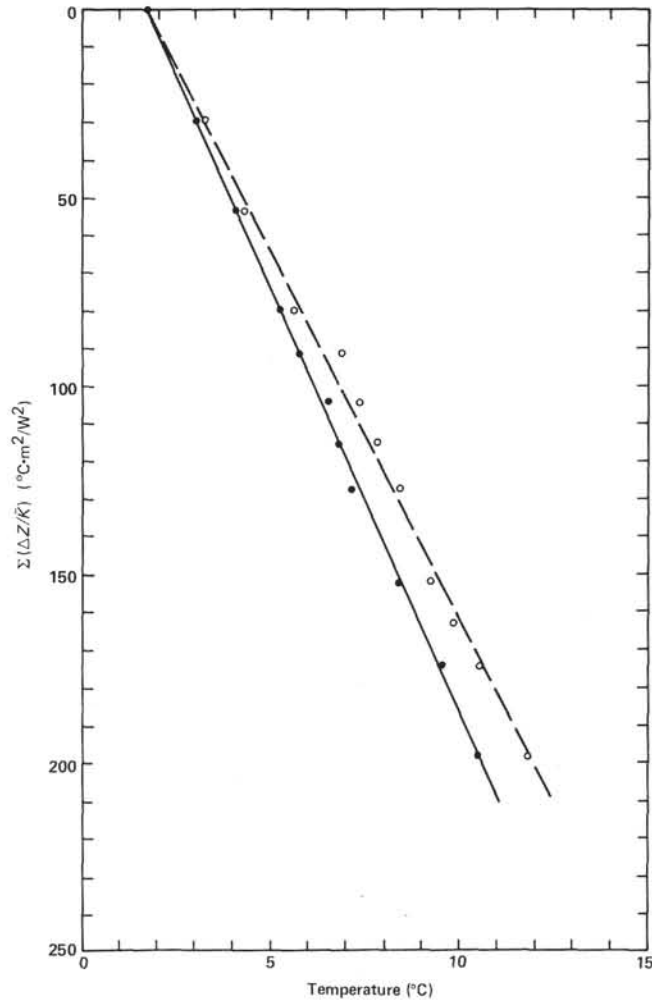


Figure 22. Plot of sediment temperatures, T_{\max} and T_{\min} , against cumulative thermal resistance at Site 580.

Table 3. Result of heat flow measurement by DSDP Leg 86.

Site	Position		Magnetic lineation	Lithospheric age (m. y.)	Heat flow (mW/m ²)	
	(N)	(S)			Q_{\max}	Q_{\min}
576	32°21.37'	164°16.53'	M13	129	61.2	56.0
577	32°26.52'	157°43.40'	(M19)	(142)	44.1	39.2
578	33°55.56'	151°37.74'	M17	137	52.9	42.7
579	38°37.68'	153°50.17'	M10	122	49.7	44.1
580	41°37.47'	153°58.58'	M 3	114	51.4	44.4

Note: Data of questionable quality are in parentheses.

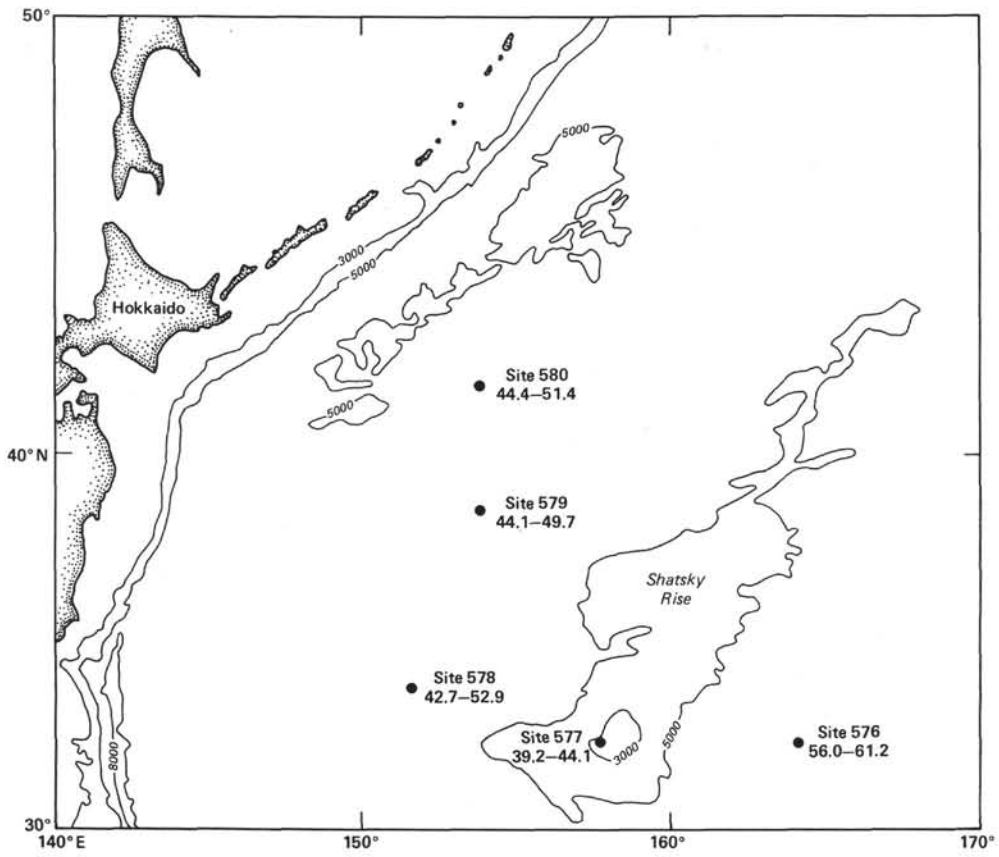


Figure 23. Geographical distribution of heat flow stations of Leg 86. Values of heat flow, $Q_{min} - Q_{max}$, in mW/m^2 ; bathymetry in meters.

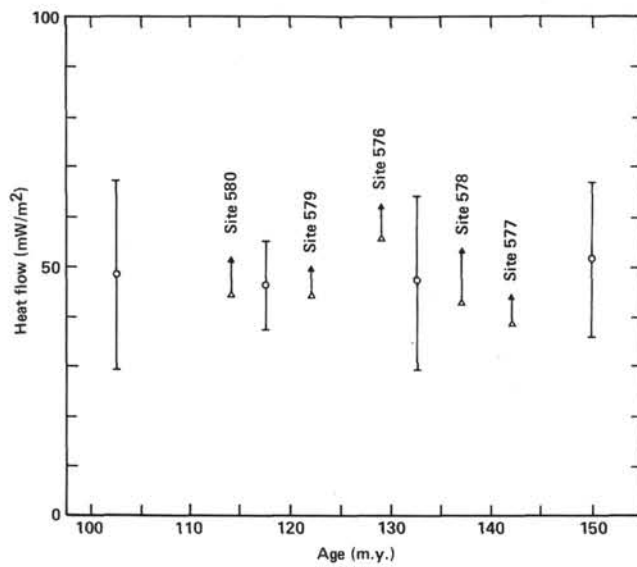


Figure 24. Heat flow versus lithospheric age relation for Leg 86 data compared with the average for North Pacific (Sclater et al., 1980).